

CARBON AND NITROGEN REDISTRIBUTION IN WELD JOINTS OF HEAT RESISTANT STEELS

Jiří Sopoušek – Masaryk University of Brno, Faculty of Science, Czech Rep.

Rudolf Foret – Brno University of Technology, Faculty of Mechanical Engineering, Czech Rep.

ABSTRACT

The present contribution deals with the theoretical modelling of the kinetics of the development of chemical composition and phase profiles of heterogeneous laboratory weld joints of heat resistant steels from the point of view of their long-term stability. The T25 (6 CrMoV 8-3-2) heat-resistant ferritic steel currently being developed and the advanced P91 (X10CrMoVNb 10-1) chromium steel, both steels after ion nitriding, homogenisation at 1050°C and weld joining were the subject of study. The basic compositions of materials were approximated as the Fe-Cr-Ni-Mo-V-C-N system. The long-term annealing of the T25+0.1129wt%N | P91+(0.8-0.064wt)N weld joints were simulated at 600°C and 900°C. The simulated results were compared with experimental carbon profile observations. The phase diagrams of the investigated materials were calculated using the CALPHAD approach [1] and applying the STEEL thermodynamic database [2]. The activities of carbon, nitrogen, and other elements were calculated by the same method. The CALPHAD approach complemented with an appropriate diffusion model [3] given in the DICTRA code enabled simulating the phase and element profile evolutions inside the diffusion-affected zone of weld joint. The DIF kinetic database [4] was used to describe the diffusion. In the simulation the coexistence of different phases (carbides, carbonitrides,...) was assumed.

KEYWORDS

CALPHAD, diffusion, carbide, carbonitride, transformation.

INTRODUCTION

Heterogeneous welds of heat-resistant steels under external stress represent an important critical point in technical applications at elevated temperatures. In many cases, the long-term mechanical stability of the weld is decisive for overall service life of the whole design solution. The mechanical stability is in close relation to the structural stability, which is given also by thermodynamic stability of the fine carbide/carbonitride phases used for precipitation hardening of heat-resistant steels.

The long-term resistibility of the manufactured welds and weld deposits represents a complicated problem, which cannot be solved en bloc but now it is possible to subdivide it into partial problems. The manufactured weld can be separated into a minimum of two separate parts, with each of them involving only one material melting zone. Two weld joints can substitute the separate parts in laboratory conditions or in PC simulation. The long-term degradation process of heat resistant steel is frequently controlled by diffusion at elevated temperatures. In such a case the weld joints can be approximated as diffusion couples and, for example, the standard approach given in [1], [3], [4], [5] can be used.

1. EXPERIMENT

Only a part of the experimental results, which will be published at EUROMAT 2005 [6] and elsewhere, is used in this paper in order to check the theoretical results presented. The shortened experimental procedure is as follows.

Samples of coin-like shape (about 4 mm in width and 12mm in diameter) were prepared from the T25 ferritic steel being developed and from the advance P91 chromium steel (see **Table 1** for initial composition). The samples were ion-nitrided and homogenized at 1050°C for 24h. A subsequent analysis of the nitrided samples (materials T25+N and P91+N) informs us that the homogenization was successful in the case of material T25+N but not for P91+N (see **Table 1**). The nitrogen content in the P91+N material remained higher on the surface after homogenization and the exponential function given in **Table 1** fits best the experimental over-all nitrogen content in P91+N (nitride case and bulk).

Table 1: Chemical compositions of the initial steels P91 and T25 and nitrided materials T25+N and P91+N. N^* gives the nitrogen content in initial steels, N^{**} represents the nitrogen content in the nitrided material, x in mm gives the distance from the surface for the P91+N material.

Wt%	C	Mn	Si	P	S	Cr	Mo	V	W	B	Al	N^*	Nb	N^{**}
T25	0.06	0.42	0.34	0.012	0.011	1.91	0.31	0.22	0.01	0.003	0.009	0.024	0.058	0.1129
P91	0.12	0.38	0.44	0.010	0.003	9.96	0.89	0.22	-	-	0.010	0.069	0.07	$0.80 \cdot e^{(-1.830x)}$

The samples of the T25+N material were individually joined with the nitrided samples of the P91+N material by electric discharge welding, and heat-treated under different conditions. Experimental results presented in this paper are those obtained for 600°C/240h and 900°C/18h.

2. EQUILIBRIUM PREDICTIONS

The CALPHAD approach [1] and the STEEL thermodynamic database [2] were used for the solution of both local and global phase equilibrium problems concerning the initial steels (T25, P91), nitrided materials (T25+N, P91+N), and weld joints ((T25+N) | (P91+N)). The approach enables the calculation of chemical compositions of equilibrated phases at a given temperature as well as any of the phase diagram cross-sections for these steels and materials. Also important is the possibility to calculate the chemical potentials/activities of elements too. A detailed description of the method used is given in [4], [7], [8], [9].

The initial steels, nitrided materials, and joints were approximated as the Fe-Cr-Mo-V-N-C thermodynamic system (compare **Table 1**). It is possible to extend the system with Mn, Ni and Si but it has no significant influence on the simulation results in this case. Niobium has a specific role. It is known that this element forms very stable niobium nitrides or carbonitrides. We may assume that niobium appears immediately during steel manufacturing as nitride, which does not change during all experimental procedures. It was assumed in our simulation that Nb could be excluded from the simulation, and the decrease in nitrogen due the niobium nitride formation could be neglected. The last two elements, S and P, were also excluded from all calculations and simulations. The phases, which can be found in the system, are different and the thermodynamic description is given in [4]. A list of phases is given in **Table 2**, which also gives the abbreviations used for phases in this paper.

Table 2: Phase abbreviations used.

phase	austenite	ferrite	M ₂₃ C ₆	M ₇ C ₃	cementite	M ₆ C	Laves phase	M ₂ X carbonitride	MX carbonitride
Abr.	FCC	BCC	M23	M7	M3	M6	LAVES	M2	MX

The calculated stable phase diagram cross-sections for the initial T25 and P91 steels, whose composition is given in **Table 1**, and for nitrated T25+N and P91+N materials are given in **Figs 1-4**. Among other facts, the temperature of phase transformations can be distinguished in **Figs 1-2** for the initial T25 and P91 steels. An important difference can be found when comparing **Fig. 3** and **Fig. 4**. It can be seen that the T25 steel and T25+N material have stable phase structures including the BCC+M7+MX phases. On the other hand, the stable phase structure of the P91 steel and that of the surface of the P91+N material with 0.8wt% of N are different (i.e. (BCC+MX+M23) versus (BCC+MX+M2)). The difference is given by the nitrogen content. The BCC+MX+M2 phases are predicted on the surface of the P91+N material, the BCC+MX+M23 phases are assumed to be deep in the P91+N material, and the BCC+MX+M23+M2 phases are assumed to coexist at a certain distance from the P91+N material surface.

Fig. 1: Phase diagram for initial T25 steel. Red line represents carbon content. Phase fields: 1...BCC+MX, 2...BCC+MX+M23+M7, 3... BCC+MX+M7+M6, 4...BCC+MX+M6, 5...BCC+MX+M23+M6.

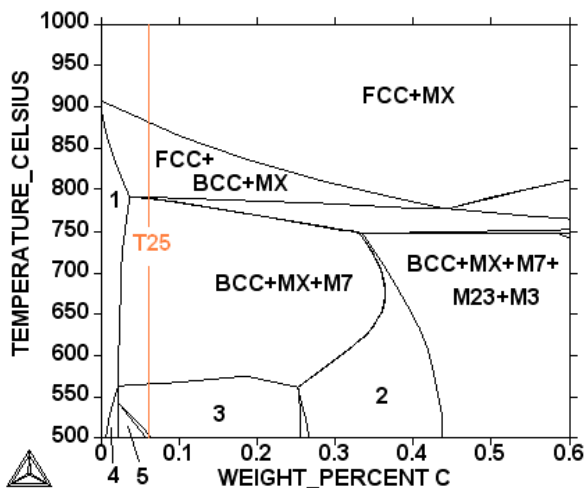
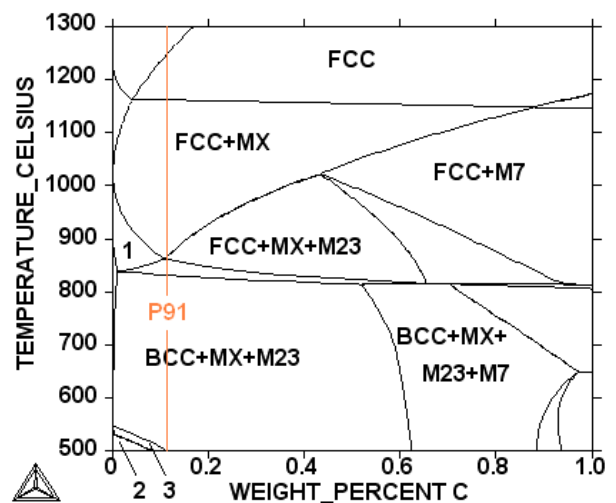


Fig. 2: Phase diagram for initial P91 steel. Red line represents carbon content. Phase fields: 1...BCC+FCC+MX, 2...BCC+MX+M6+LAVES, 3...BCC+MX+M6+M23.



An important result of phase equilibrium calculations and predictions is the evaluation of the activities of individual elements in the steels and nitrated materials with respect to standard element reference (SER) [10]. The activity difference of the given element in two different materials can be used as a rough approximation for weld joint stability judgement [5] because each element diffuses to a place with its lower activity and this diffusion flux is roughly proportional to the absolute value of the activity difference. In the case of the microstructure evolution of weld joints of the materials based on nitrated steels, carbon and nitrogen are of most importance because they diffuse most quickly and thus the diffusion of the metal elements can be neglected.

The temperature dependences of the carbon activity for the examined initial steels under and nitrated materials are given in **Fig. 5**. Here it is shown how the temperature and the nitriding influence the carbon activity. In spite of the higher carbon content (0.12wt%) in the P91+N material and the lower carbon content (0.06wt%) in the T25+N material, making a couple from these materials given in **Fig. 5** shows that the carbon will diffuse from T25+N to P91+N at low

temperatures, ranging from 500-870°C (i.e. carbon up-hill diffusion). A special effect - no diffusion - can be expected in the case that we join two alloys of the same carbon activities (see crossing of the lines for T25+0.1129wt%N and for P91 at ca. 870°C in **Fig. 5**, as a theoretical example).

The carbon mass transport is much more intensive than the nitrogen transport in both the T25+N and the P91+N materials. The calculated nitrogen activity differences for diffusion couples of the initial steels and nitrided materials are very low (10^{-10} - 10^{-7}) [4]. The nitrogen mass transport does not play a great role in the T25+N | P91+N joints in the monitored temperature range.

Fig. 3: Isothermal section (at 600°C) of phase diagram of Fe-Cr-Mo-V-C-N system at constant metal composition given in **Table 1** for T25. Crosses show carbon and nitrogen contents of initial T25 steel (+) and nitrided T25+N steel (+). Phase fields: 1...BCC+MX+M23+M7, 2...BCC+MX+M23.

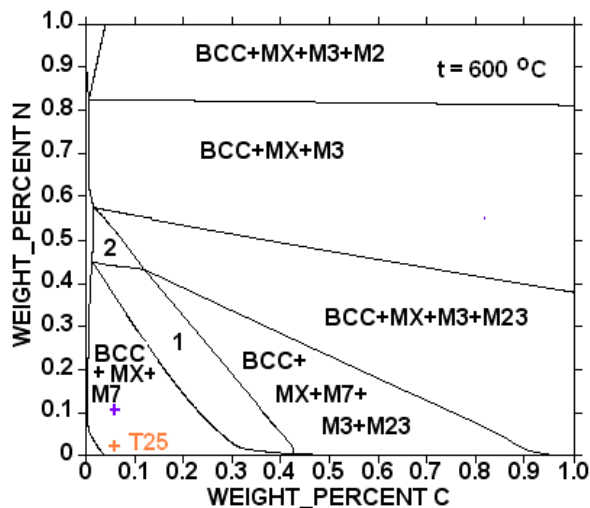
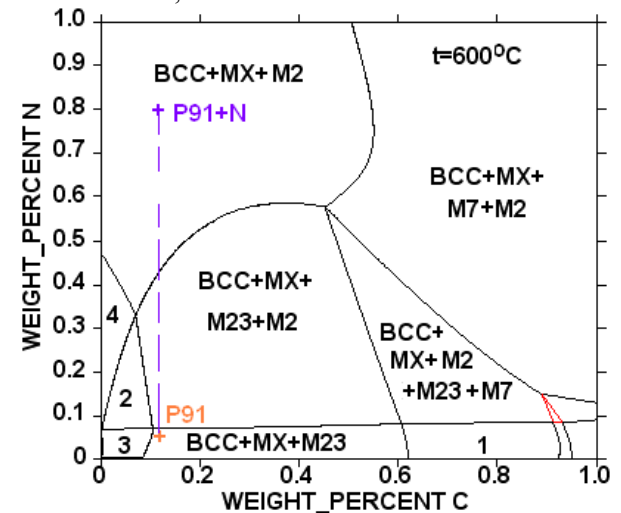


Fig. 4: Isothermal section (at 600°C) of phase diagram of Fe-Cr-Mo-V-C-N system at constant metal composition given in **Table 1** for P91. Crosses show carbon and nitrogen contents of initial P91 steel (in red: P91) and of P91+N nitride case (in blue: P91+N). Phase fields: 1...BCC+MX+M23+M7, 2...BCC+MX+M23+M2+LAVES, 3...BCC+MX+M23+LAVES, 4...BCC+MX+LAVES+M2.



3. DIFFUSION SIMULATIONS

Two heat-treated T25+N | P91+N weld joints (experiments at 600°C/240h and 900°C/18h) were simulated as two dissimilar Fe-Cr-Mo-V-C-N systems being in diffusion contact (as the so-called diffusion couples). The melting zone width was put to zero and step-like overall initial element profiles were assumed for all elements excluding the nitrogen in accordance with **Table 1**. The DICTRA programme [11] [12], which contains subroutines for the CALPHAD method [1], was used as a tool for such simulations.

The benefits of using the DICTRA program are described in [3] and [13]. This programme embodies the assumption of local condition of phase equilibrium, the assumption that diffusion is the controlling process of the phase transformation rate [14] [15], the theory of multi-component bulk diffusion [16] and, of course, the gradients of chemical potentials/activities of the elements are considered for mass flux evaluations. The individual diffusion couples were treated by the same approach as described in [4] or [5]. The diffusion matrix formed from the BCC (at 600°C) or the FCC (at 900°C) phase was assumed.

The other phases (see **Table 2**) were treated as diffusionless phases in local phase equilibrium with the appropriate diffusion matrix. The STEEL thermodynamic database [2] and the DIF kinetic database [4] were used for the simulations of the T25+N | P91+N weld joints at temperatures of 600°C and 900°C. The simulation results were visualised on profiles showing the dependence of selected values (molar fractions of phases, overall concentrations of elements, phase composition) on distance at a chosen time (see **Fig. 5-14**).

Fig. 5: Simulated temperature dependence of carbon activity of investigated initial steels and nitrided materials.

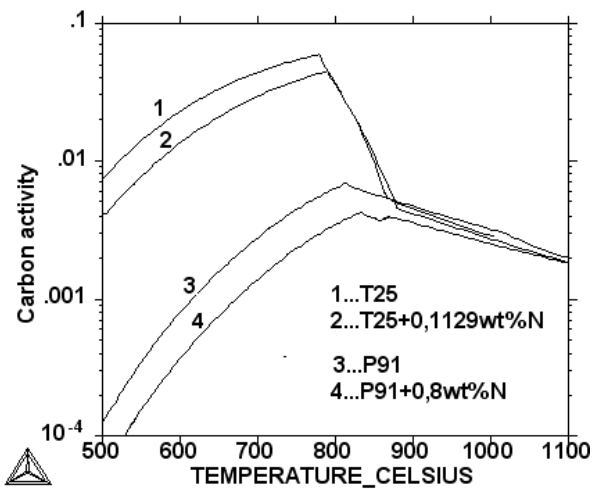
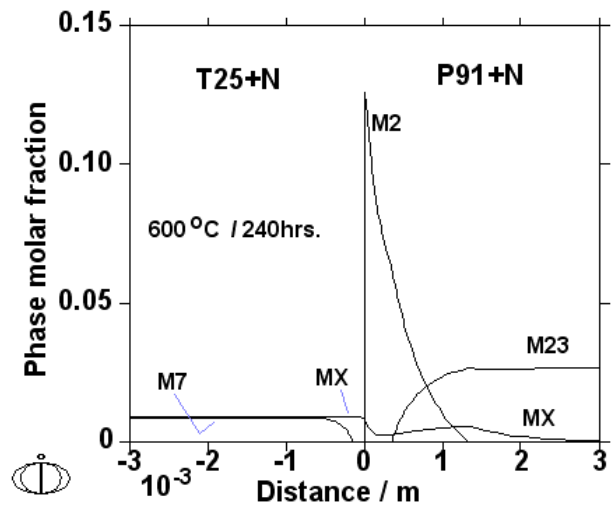


Fig. 6: Simulated phase profiles of T25+N | P91+N weld joints after annealing at 600°C/240h.



The results of the simulation at 600°C/240h are given in **Figs 6-12**. The carbon up-hill diffusion can be observed at this temperature. The carbon diffused from the T25+N material to the P91+N material in accordance with the carbon activity difference given in **Fig. 5**. The carbon depleted zone inside the T25+N material and the carbon enriched zone inside the P91+N material are formed in the vicinity of the T25+N | P91+N weld joint interface. **Fig. 6** shows the M7 chromium rich carbide dissolution given by the displacement of carbon from the T25+N material. The carbon overflow replaces nitrogen in M2 carbonitride in the P91+N material. The nitrogen diffusion is very slow and the initial nitrogen profile remains stable. The high thermodynamic stable MX carbonitride can be found in the carbon depleted as well as in the carbon enriched zones. The M2 carbonitride can be found in the P91+N material with high nitrogen content (in the position of the original nitride case). The compositions of the carbonitride and carbide phases varied with distance and they are given in **Figs 7-10**. The matrix composition profile after annealing 600°C/240h can be taken from **Fig. 11**. The simulated and experimental carbon profiles can be found in **Fig. 12**.

Fig. 7: Simulated MX phase composition profiles of T25+N | P91+N weld joint after annealing 600°C/240h.

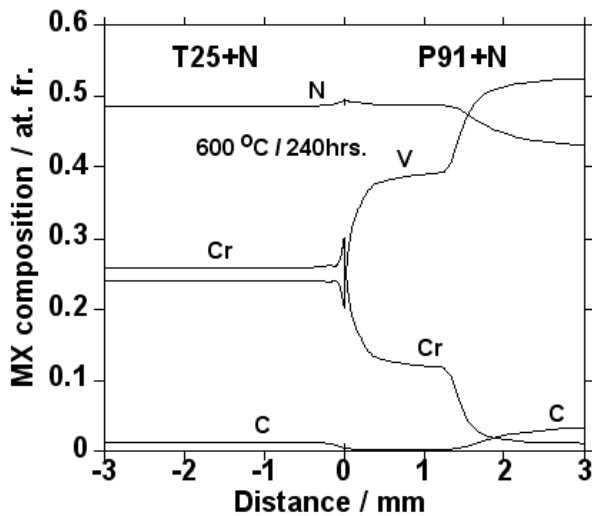


Fig. 9: Simulated $M_{23}C_6$ phase composition profiles of T25+N | P91+N weld joint after annealing 600°C/240h.

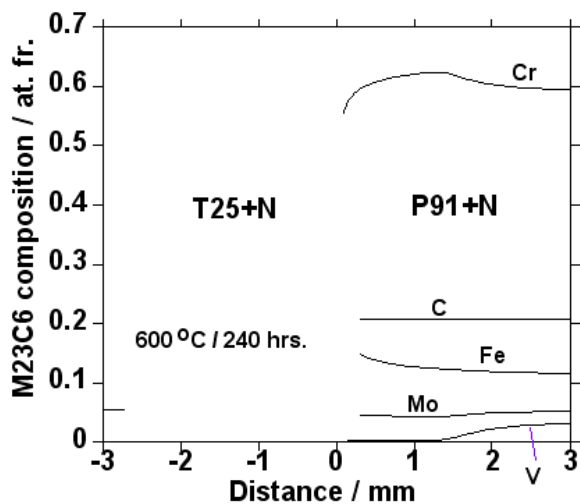


Fig. 8: Simulated M_2X phase composition profiles of T25+N | P91+N weld joint after annealing 600°C/240h.

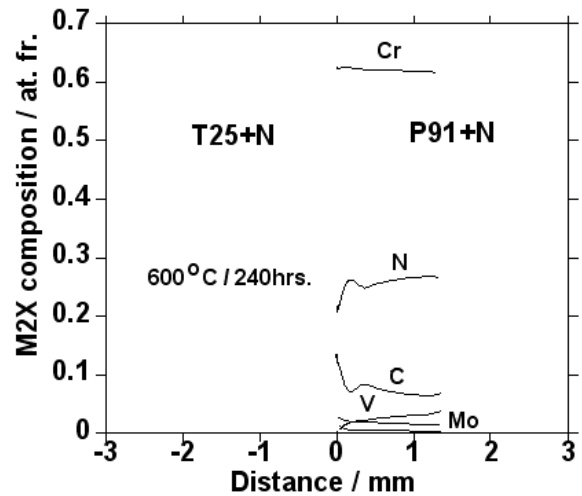
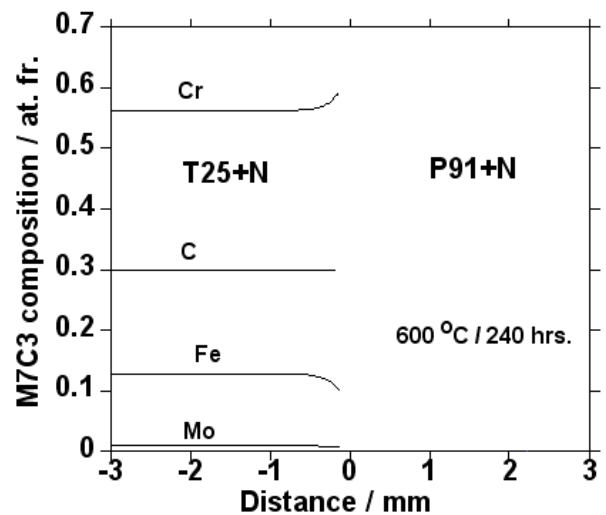


Fig. 10: Simulated M_7C_3 phase composition profiles of T25+N | P91+N weld joint after annealing 600°C/240h.



Figs 13-15 refer to simulation results at 900°C. The carbon diffusion can be neglect in the T25+N | P91+N diffusion couple (consider carbon activity from Fig. 5). Fig. 13 shows that the MX carbonitride could be present in the weld joint at 900°C only. The MX molar phase fraction is fixed in accordance with the initial nitrogen content. The compositions of the MX carbonitride varied with distance as shown in Fig. 14 and the simulated carbon profile can be found in Fig. 15.

4. DISCUSSION

The phase diagrams calculated and presented in Figs 1-4 can be used for better understanding the phase structure of the steels and materials under study. The phase field boundaries drawn on iso-concentration and iso-temperature phase diagrams show the stable regions with coexisting phases (carbides, carbonitrides) and can be used for heat treatment design. One point should be noted concerning Fig. 4, where it is possible to see that the M23 carbide can be replaced by the M2 carbonitride in the P91 advanced alloy with extra high nitrogen content.

Fig. 11: Simulated profiles of composition of BCC diffusion matrix of T25+N | P91+N weld joint after annealing 600°C/240h.

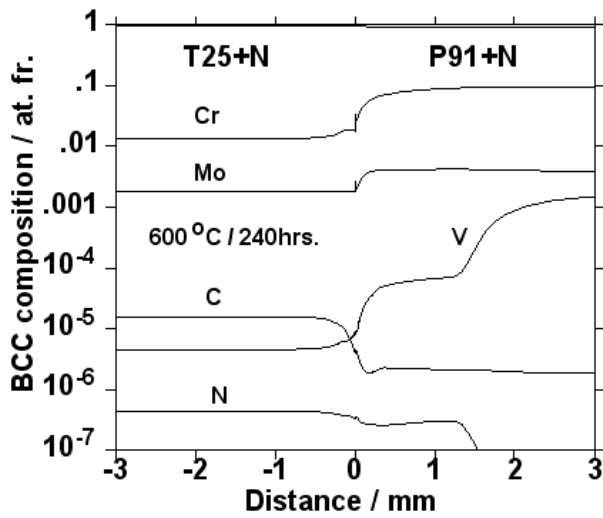


Fig. 13: Simulated phase profile of T25+N | P91+N weld joint after annealing 900°C/18h.

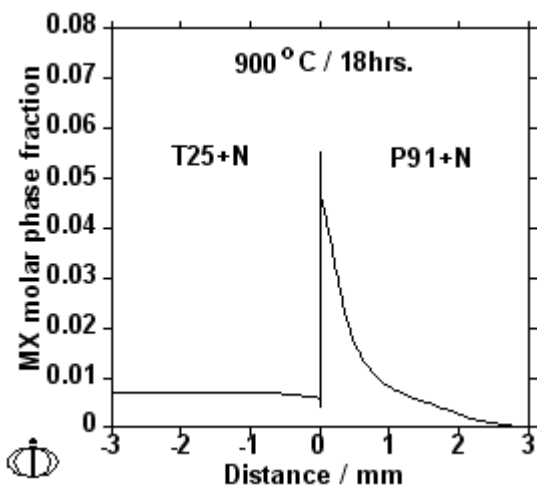


Fig. 12: Simulated bulk carbon profiles of T25+N | P91+N weld joint after annealing 600°C/240h. Experiment

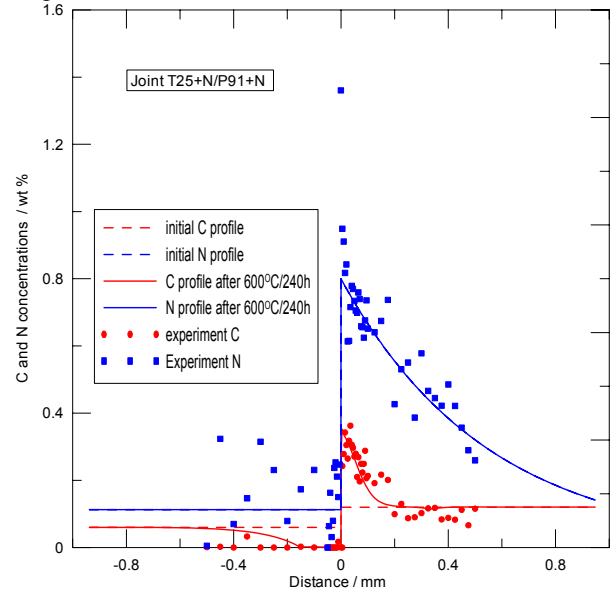
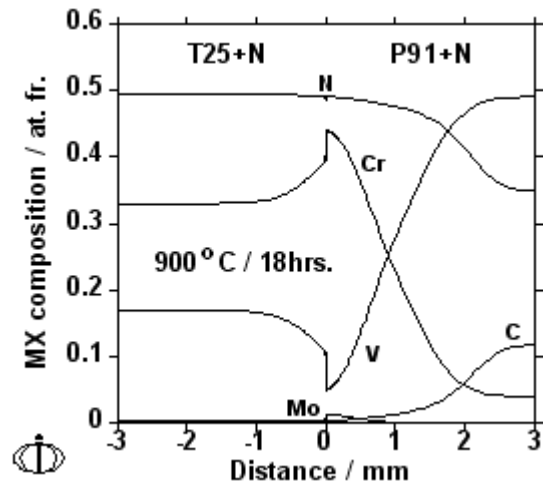


Fig. 14: Simulated MX phase composition profiles of T25+N | P91+N weld joint after annealing 900°C/18h.

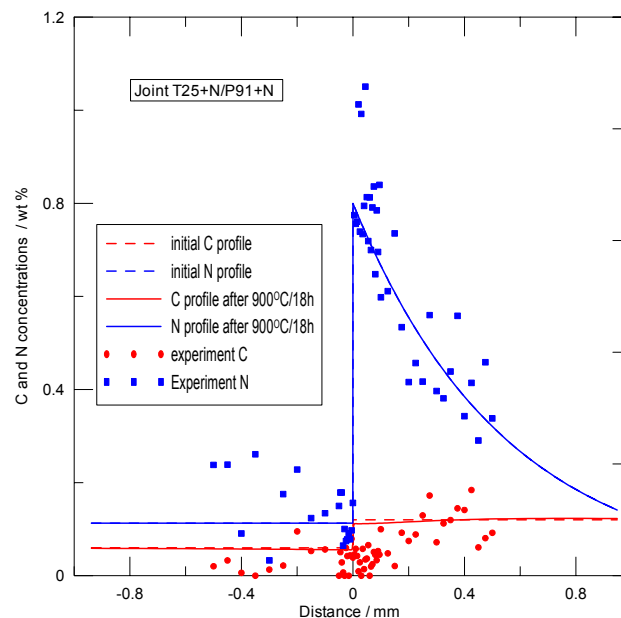


The thermodynamic and kinetic stability of the weld joints of dissimilar materials can be estimated from the carbon activity temperature dependence similar to that given in **Fig. 5**. More precise results can be attained on the basis of weld joint simulations described in this paper (see **Figs 5-15**). The simple knowledge of the activity dependences is sometimes sufficient to estimate the effect of nitrogen on weld stability of heat resistant steels. In our case the nitriding decreases the carbon activities of both the T25 and the P91 ferrite steels (see **Fig. 5**). From the thermodynamic point of view the nitriding of the advanced P91 steel is a wrong experimental procedure here because it does not retard the carbon depleted zone evolution in the T25+N material and, moreover, carbon depleted zone occurs in the neighbourhood of P91+N material region strengthened with M2

carbonitride. Regardless of this, from the theoretical point of view it is quite an illustrative example for study.

A correct judgement of the weld stability of heat resistant steels alloyed with carbon and nitrogen is not possible on the basis of carbon activity temperature dependence alone but it is necessary to perform more precise kinetic simulations. The simulations performed for the T25+N | P91+N weld joint show a great difference in the diffusion and phase stability at 600°C (**Figs 6-12**) and at 900°C (**Figs 13-15**). The T25+N | P91+N diffusion joint reveals the formation of carbon depleted zone and carbon enriched zone at 600°C, which is confirmed by the experiment given in **Fig. 12**. This weld joint combination represents much risk in practical service conditions at 600°C. High diffusion stability is reached at 900°C. The diffusion is negligible at this temperature but it has to be noted that the matrix is formed by the FCC phase (austenite) at this temperature, which is above the temperature range of the applications of the steels under study. The diffusion stability at 900°C is experimentally confirmed in **Fig. 15**.

Fig. 15: Simulated bulk carbon profiles of T25+N | P91+N weld joint after annealing 900°C/18h. Experiment values added.



5. CONCLUSION

The simulation results enable understanding the processes taking place in the diffusion-affected zone of the studied weld joint under different temperature conditions. It was found that the nitriding of both heat resistant steels decreased their carbon activities. This decrease is desirable for the T25 steel but useless for the P91 steel. The kinetic simulation of the T25+N | P91+N weld joint has confirmed it. It can be concluded that the method used provides results that are in good agreement with experimental observations.

The STEEL thermodynamic database [2] and the DIF kinetic database [4] were used for the simulation of the simultaneous diffusion of carbon and nitrogen. The simulation results obtained not only in this paper but also for other weld combinations of heat resistant steels show good agreement with experiments. The results obtained show that the databases can be used for the design of welds of heat resistant steels.

The simulation procedure used can be transferred to weld joints of heat resistant steels with simultaneous carbon/nitrogen diffusion. In this case, the simulation method can offer results that can be used for the evaluation of long-term microstructural stability of weldments at high temperatures.

ACKNOWLEDGEMENT

The support of the Grant Agency of the Czech Republic (project No. 106/03/0636) and Ministry of Education, Youth and Sports (project No. MSM/0021622410) is gratefully acknowledged.

REFERENCES

- 1) N. SAUNDERS and A. P. MIODOVNIK, CALPHAD (calculation of phase diagram) – A Comprehensive Guide, Elsevier Science, Amsterdam (1998).
- 2) A. KROUPA, J. HAVRÁNKOVÁ, M. COUFALOVÁ, M. SVOBODA, and J. VŘEŠŤÁL, Journal of Phase Equilibria, 22/3, (2001), pp. 312-323.
- 3) A. BORGSTAM, A. ENGSTRÖM, L. HÖGLUND, J. ÅGREN, J. of Phase Equilibria, 21/3, (2000), pp. 269-280.
- 4) J. SOPOUŠEK, V. JAN, and R. FORET, Science and Technology of Welding and Joining, 9/1, (2004), pp. 59-63.
- 5) V. JAN, J. SOPOUŠEK, R. FORET, Archives of Metallurgy and Materials, 49/3, (2004), pp.439-480.
- 6) R. FORET, J. BURŠÍK, J. SOPOUŠEK, EUROMAT 2005, 5-8 September, Prag.
- 7) B. SUNDMAN AND J ÅGREN, J. Phys. Chem. Solids, 42, (1981), pp. 297-301.
- 8) M. HILLERT, Phase equilibria, Phase Diagrams and Phase Transformations – Their Thermodynamic Basis, Cambridge University Press, (1998).
- 9) I. ANSARA and B. SUNDMAN, CALPHAD, 24, (2000), pp. 181-182.
- 10) A. T. DINSDALE, CALPHAD, 15, (1991), pp. 317-425.
- 11) J. O. ANDERSON, T. HELANDER, L. HÖGLUND, P. F. SHI, B. SUNDMAN, CALPHAD, 26, (2002); 273-312.
- 12) http://web.mse.kth.se/~lars/users_guide.pdf (dated 25.6.2005).
- 13) <http://web.mse.kth.se/~lars/examples.pdf> (dated 25.6.2005).
- 14) J. S. KIRKALDY, D. J. YOUNG, Diffusion in the Condensed State, The Institute of Metals, London (1985).
- 15) A. ENGSTRÖM, L. HÖGLUND, J. ÅGREN, Metall Mater Trans, 25A, (1994), pp. 1127-1134.
- 16) J. O. ANDERSSON, L. HÖGLUND, B. JÓNSSON, J. ÅGREN, In: G. R. Purdy editor. Fundamentals and Applications of Ternary Diffusion, Pergamon Press, New York (1990), p 153.